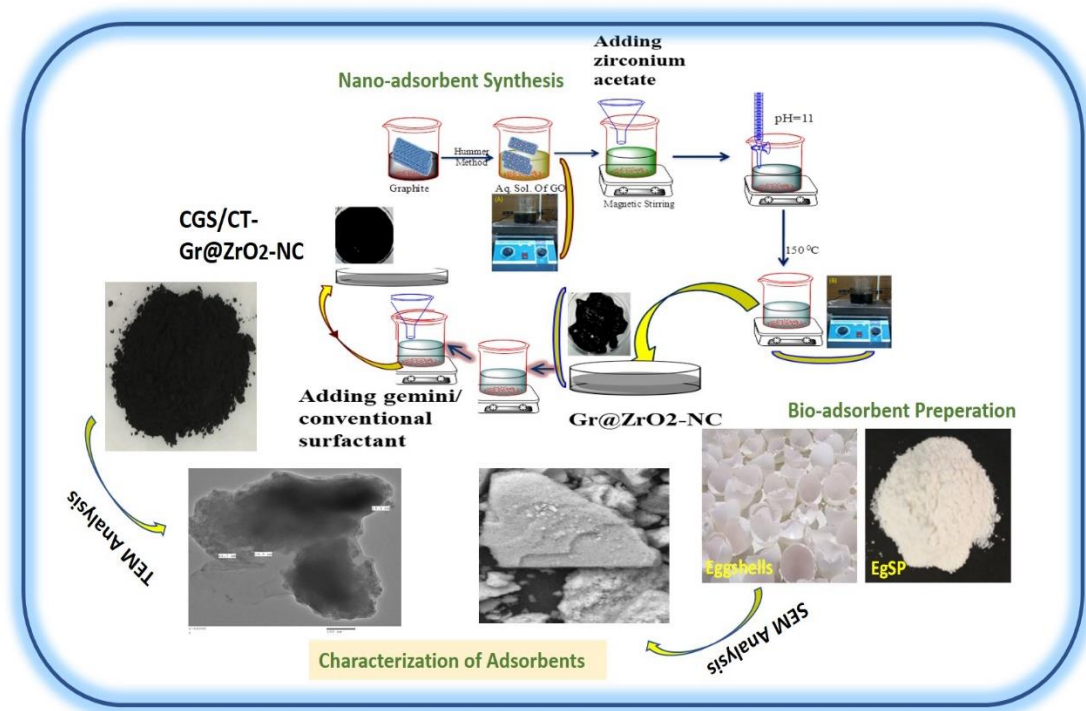


Chapter 2

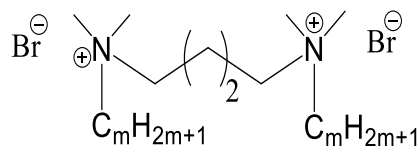
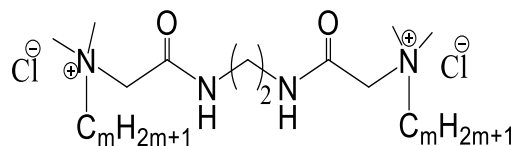
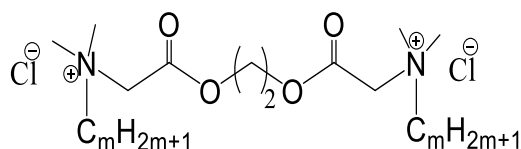
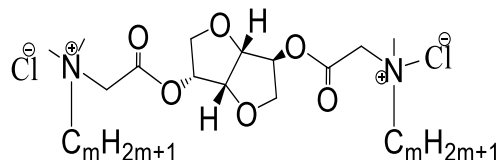
Materials and Methods



2.1. Materials

Gemini surfactants are synthesized and characterized by reported procedure [1-3]. Molecular structures of geminis with acronyms are given in Scheme 1 and Table 1, respectively. 1,4-dibromobutane (99%, Sigma Aldrich), ethylene glycol (99%, Sigma Aldrich), ethylenediamine (99%, S.d.Fine Chemicals), D-Isosorbide (99%, Sigma Aldrich), chloroacetylchloride (CAC, 98%, S.d.Fine Chemicals, used after simple distillation), *N,N*-hexadecyldimethyl-1-amine (95%, Sigma Aldrich), *N,N*-tetradecyldimethyl-1-amine (95%, Sigma Aldrich) and *N,N*-dodecyldimethyl-1-amine (95%, TCI Chemicals), triethyl amine (99%, spectrochem), n-dodecenol (98%, SISCO), pyrophosphoric acid (>90%, Fluka), 25% methanolic solution of tetramethylammonium hydroxide (Sigma Aldrich), sodium metal (95%, Loba), sodium hydroxide (99.5%, Merck), concentrated hydrochloric acid (Spectrochem), Surface active ionic liquid (SAIL, Tetrapentylammonium bromide, Sigma Aldrich), Cetyltrimethylammonium bromide (Sigma Aldrich) Glycine, (Sigma Aldrich), β -cyclodextrin (Spectrochem, Mumbai, India), Methyl orange, Congo Red (Loba Chemie Pvt. Ltd Mumbai, India), Graphite Powder (Loba Chemie Pvt. Ltd Mumbai, India.), Zirconium acetate (Sd Fine Chemicals) are used as received. All organic solvents (dichloromethane (DCM), toluene, acetonitrile, diethyl ether, chloroform, methanol, dry ethylacetate) were purchased as AR grade from spectro-chem and used as received. Absolute alcohol (99.5%) was provided by Applied Chemistry Department, The Maharaja Sayajirao University of Baroda, India (Gujarat government approved). Absolute ethanol was dried by using of magnesium / iodine and stored on molecular sieves. Freshly prepared de-ionized double distilled water ($\kappa=0.5-1.5\mu\text{S}\cdot\text{cm}^{-1}$) was used to prepare the solution for all measurements except SANS and NMR studies, where, D₂O has been used in the sample preparation.

Cationic Gemini Surfactants

*m-4-m**m-Eda-m**m-Eg-m**m-Isb-m*

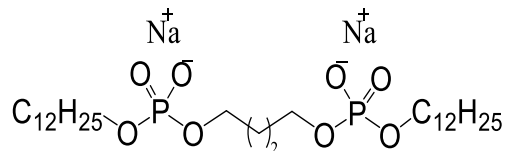
m-4-m; where, m = 12, 14, 16

m-Eda-m; where, m = 12, 14, 16

m-Eg-m; where, m = 12, 14, 16

m-Isb-m; where, m = 12, 14, 16

Anionic Gemini Surfactant



12-4-12 A

Scheme 1. Schematic representative chemical structures of anionic and cationic gemini surfactants.

Table 1. Cationic Gemini surfactants with their acronyms.

Sr. No.	Cationic Gemini Surfactant	Acronyms
1.	Butanediyl-1,4- bis(N,N-dimethyl-N-hexadecyl-ammonium) dibromide	16-4-16
2.	Butanediyl-1,4-bis(N,N-dimethyl-N-tetradecyl-ammonium) dibromide	14-4-14
3.	Butanediyl-1,4-bis(N,N-dimethyl-N-dodecyl-ammonium) dibromide	12-4-12
4.	D-isosorbate-1,4-diyl bis(N,N-dimethyl-N-hexadecyl-ammonium acetoxy) dichloride	16-Isb-16
5.	D-isosorbate-1,4-diyl bis(N,N-dimethyl-N-tetradecyl-ammonium acetoxy) dichloride	14-Isb-14
6.	D-isosorbate-1,4-diyl bis(N,N-dimethyl-N-dodecyl-ammonium acetoxy) dichloride	12-Isb-12
7.	Ethane-1,2-diyl bis(N,N-dimethyl-N-hexadecyl-ammonium acetoamide) dichloride	16-Eda-16
8.	Ethane-1,2-diyl bis(N,N-dimethyl-N-tetradecyl-ammonium acetoamide) dichloride	14-Eda-14
9.	Ethane-1,2-diyl bis(N,N-dimethyl-N-dodecyl-ammonium acetoamide) dichloride	12-Eda-12
10.	Ethane-1,2-diyl bis(N,N-dimethyl-N-hexadecyl-ammonium acetoxy) dichloride	16-Eg-16
11.	Ethane-1,2-diyl bis(N,N-dimethyl-N-tetradecyl-ammonium acetoxy) dichloride	14-Eg-14
12.	Ethane-1,2-diyl bis(N,N-dimethyl-N-dodecyl-ammonium acetoxy) dichloride	12-Eg-12

2.2. Synthesis of Gemini Surfactants

2.2.1. Cationic Gemini Surfactants

Gemini surfactants (GS) with different alkyl chain length ($m = 12, 14$ or 16) and spacers have been synthesized and characterized using various physical and spectroscopic techniques. Spacers (1,4-dibromobutane, 1,2-bischloroacetylinediamine, 1,2-bischloroacetoxyethane and 1,4-bischloroacetoxy-D-isosorbate) and various alkyl quaternary amines (*N,N*-dimethyldodecyl-1-amine, *N,N*-dimethyltetradecyl-1-amine and *N,N*-dimethylhexadecyl-1-amine) are mixed (in an appropriate ratio) with dry ethylacetate- DCM or dry ethanol- ethylacetate or dry ethanol in 250 ml round bottom flask and refluxed for 24 to 48 h (under N_2 atmosphere with guard tubing).

2.2.2. Anionic Gemini Surfactant-(*Phosphoric acid, P, P'-1,4-butanediyl, P, P' didodecylester, disodium salt, 12-4-12A*)

12-4-12 A has been prepared in two steps [4-6]: 1) dodecyl dihydrogenphosphate has been obtained by mixing *n*-dodecanol and pyrophosphoric acid in toluene (10-20 ml). Stirring continued till clarity and then the mixture was kept for 4 days. The resulting mass then dissolved in diethyl ether followed by repeated (three times) washing with water. The etherical layer was added to dilute NaOH under constant stirring. Out of the two layers (water and ether layers), ether layer has been discarded and pH of the aqueous layer was adjusted. This gives concentrated dodecyl dihydrogenphosphate; 2) dodecyl dihydrogen phosphate was mixed with methanolic solution of tetramethylammonium hydroxide at ambient temperature. After removal of methanol (under reduced pressure), the solid mass has been mixed with 1, 4-dibromobutane in acetonitrile with constant stirring followed by refluxing for 1-2 h. After removal of solvent (by applying vacuum), the resulted mass was acidified with dilute HCl followed by extraction with diethyl ether. The etherical layer was washed with water. After

removal of ether, the brownish solid was crystallized with a mixture of CHCl_3 : ethyl acetate (40:60) to obtain pure hydroxyl form of AGS. The hydroxyl form was again reacted with sodium ethoxide ($\text{C}_2\text{H}_5\text{ONa}$) in dry ethanol. After removal of ethanol, the pure AGS (12-4-12-A,) was dried under vacuum.

2.3. Synthesis and Modification of Adsorbents

2.3.1 Synthesis of GO and Gr@ZrO₂-NC

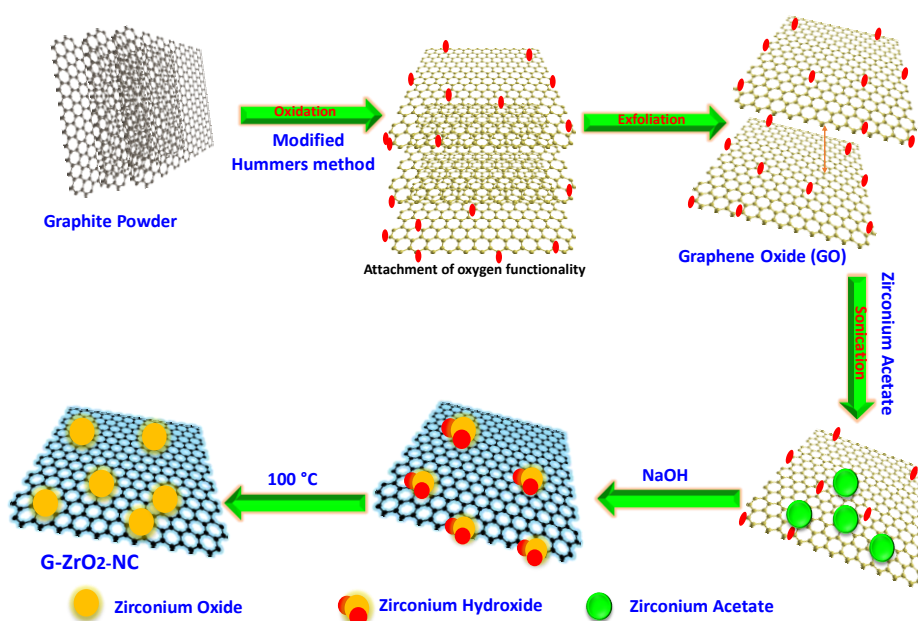
2.3.1.1. Preparation of GO

Synthesis of graphene oxide (GO) was carried out by a modified Hummer method, which involves graphite exfoliation in presence of strong acids and oxidants [7, 8]. Schematic synthesis is illustrated in Scheme 2. Mixture of H_2SO_4 , HNO_3 , and H_3PO_4 (7: 2: 1 ratio) was used to suspend graphite powder under constant stirring. KMnO_4 was slowly added in suspension kept in ice bath. After the addition, the ice bath was replaced by a water bath and suspension was stirred for another 2 h (at $\sim 40^\circ\text{C}$). Further, 200 ml water was added drop by drop to the suspension, maintaining its temperature below 90°C . In the suspension, 20 ml H_2O_2 (30% aqueous solution) was added under constant stirring. The color of the suspension was changed from brown to greenish-yellow which indicate the formation of GO. GO was washed twice with 1:10 HCl followed by repeated washing with water to neutralize pH. The decanted product was again dispersed in water followed by sonication (30 m) to get exfoliated GO. The suspension was centrifuged at 700 rpm for 20 m to remove exfoliated graphite. Subsequently, the acquired graphene oxide (GO) thick mass was dried for about 24 h in a vacuum oven at 55°C .

2.3.1.2. Synthesis of Gr@ZrO₂-NC

Synthesis of nanocomposite was carried out by sonicating the dispersed aqueous suspension of GO (1 g in 100 ml of water) for 30 m. Sonicated dispersion was stirred

with 100 ml aqueous solution of Zirconium acetate (1g) and then it was sonicated for 1h followed by the slow addition of 20 ml of 1M NaOH. The resultant mixture was stirred for another 1h at 100 °C. Change in the color (from greenish yellow to black) of precursor mixture indicates the formation of Gr@ZrO₂-NC. The black dispersion was filtered and washed with ethanol and water, subsequently. Finally, the black shiny powder of Gr@ZrO₂-NC was recovered after drying (12h) at 100 °C [9,10].



Scheme 2. Schematic representation of synthesis of Graphene oxide and graphene zirconium oxide.

2.3.1.3. Surface Modification of Synthesized Gr@ZrO₂-NC

Surfactant modified adsorbent (*CT-Gr@ZrO₂-NC* or *CGS-Gr@ZrO₂-NC*) was synthesized by stirring an aqueous dispersion of Gr@ZrO₂-NC (100 ml) (30 mg/mL) with the gradual addition of an appropriate surfactant (CTAB or CGS) solution (1 mg/mL) [6]. The resulting mixture was sonicated (5 m) followed by gentle stirring (2h) at ambient temperature. The surfactant-modified adsorbent dispersion was centrifuged

and then washed with water. The obtained modified nano-composite was dried (under vacuum at 65 °C) and stored under dark.

2.3.2. Preparation and Surfactant Modification of Eggshell Powder (CT-EgSP, CGS-EgSP)

Eggshells were collected, crushed, washed with water several times and then dried in sunlight. Dried eggshells were further powdered, sieved through 37 microns (BSS 400) sieve and again washed with distilled water till no turbidity observed in background solution. 1% (w/w) solution of CTAB or CGS, was prepared and the washed eggshell powder mixed with the solution and stand for 1h contact time. This was washed several times to remove any unbound surfactant content from the surface. The washed surfactant modified eggshell powder (CT-EgSP or CGS-EgSP) was then dried in an oven at 60 °C for 24 h and latter stored in air tight container [11].

2.4. Structural Characterization of Bio/ Nano-Adsorbents With and Without Surfactants

2.4.1. Characterization of Gr@ZrO₂-NC Based Adsorbents (With and Without Surfactant)

XRD patterns of GO and Gr@ZrO₂-NC are collected for the confirmation of composite formation (Figure 1). A peak ~ 11° ascribes to the 001 reflections of GO. However, the pattern for Gr@ZrO₂-NC contains two broad peaks at 31° and 55°, reflecting the amorphous nature of the composite. Similar patterns were observed even with surfactant-modified composites (Figure 2(a)). This indicates that the amorphous nature of the composite maintained even after its modification with conventional (CTAB) or gemini (CGS) surfactants. The absence of any impurity peak ensures the purity of the surfactant-modified composite.

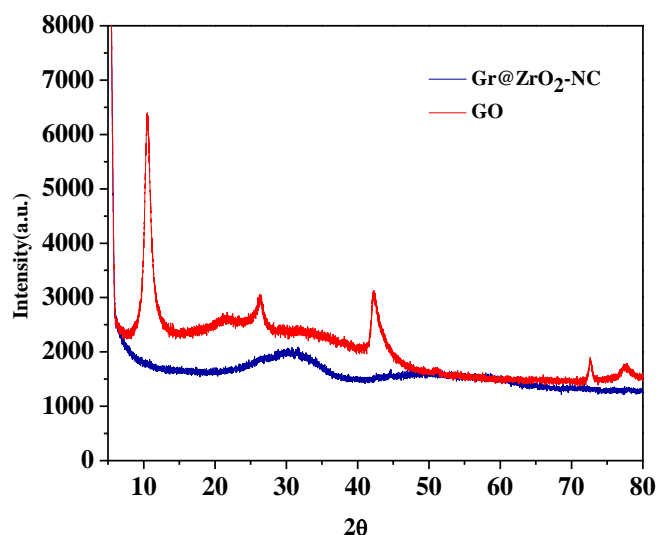


Figure1. XRD spectra of graphene oxide and graphene zirconium oxide nanocomposite.

FT-IR spectra of Gr@ZrO₂-NC, CT-Gr@ZrO₂-NC and CGS-Gr@ZrO₂-NC are shown in Figure 2b. Spectrum for Gr@ZrO₂-NC shown strong bands at 471, 944 and 1580 cm⁻¹ that can be assigned to the stretching vibrations of Zr-O, C-O and C=C functional groups, respectively. The modification of the composite was confirmed by appearance of the new peaks at 2914 and 2849 cm⁻¹ for CTAB while 2923 and 2850 cm⁻¹ for CGS, respectively. The peaks are assigned to asymmetric / symmetric stretching and scissor modes of methylene group of the alkyl tail(s). This also indicate that binding of surfactant is taking place on the surface of the composite. Compared with Gr@ZrO₂-NC, CT-Gr@ZrO₂-NC / CGS-Gr@ZrO₂-NC has a large number of hexadecyl tail chain(s) and is therefore lipophilic in nature. Stability of the adsorbent is also confirmed by TGA data (Figure 2c). It can be seen that CT-Gr@ZrO₂-NC exhibited degradation peak at a lower temperature (~120 °C) as compared to the Gr@ZrO₂-NC, which may be due to the incorporation of the surfactant moieties. On comparing the thermal stability of CT-Gr@ZrO₂-NC and CGS-Gr@ZrO₂-NC, the latter shows multiple degradation peaks. This may be due to architectural differences between the

two types of cationic surfactants. Probably, the presence of more than one alkyl tail/head group and the additional spacer may contribute a different degree of composite stability and responsible for the above-mentioned behavior. A similar type of comparative adsorption behavior of conventional and gemini surfactant has been reported for a natural adsorbent [12, 13]. The formation of graphene composite nanosheets, further confirmed by TEM images (Figure 3a-c). Compact sheet like structure of Gr@ZrO₂-NC (Figure 2a) loosened up with CT (Figure 2b). These sheets are seen fairly well separated in case of CGS modified adsorbent (Figure 2c).

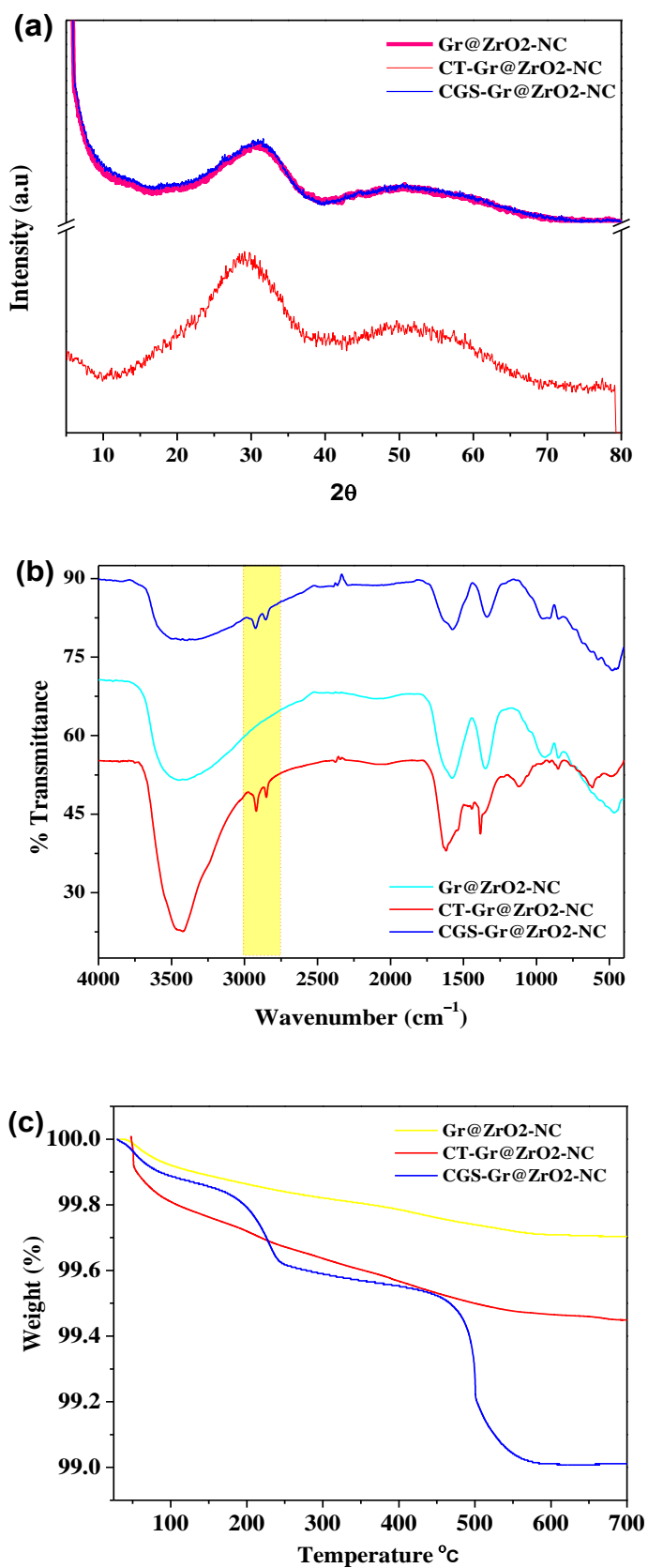


Figure 2. XRD, FTIR and TGA data for Gr@ZrO₂-NC and surfactant modified nanocomposites

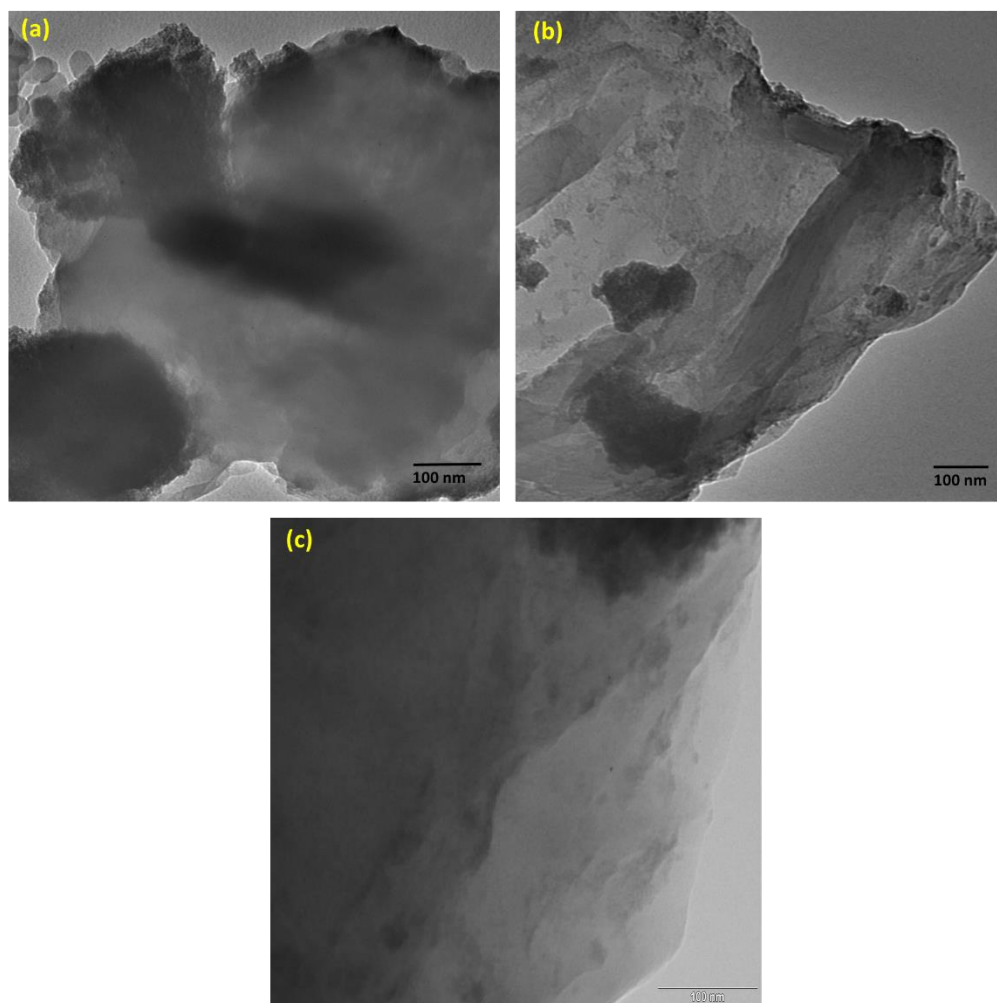


Figure 3. TEM images for Gr@ZrO₂-NC (a) and surfactant modified (b and c) nanocomposites

2.4.2. Characterization of Pure and Surfactant Modified Bio- Adsorbent (EgSP)

FTIR analysis of pure EgSP has been carried to examine the functional groups on the surface of powdered eggshells. Peaks observed (Figure 4a) at 2871, 2522, 1801, 1644, 1430, 867, and 699 cm⁻¹ are strongly associated with the presence of CaCO₃ [14]. Peaks at 3276 cm⁻¹ is observed for hydroxyl (O-H), peak at 1655 cm⁻¹ is due to carbonyl group and peak at 1171 cm⁻¹ corresponds to C-O stretching [15]. After modification of EgSP surface with surfactant, a peak at 2916 cm⁻¹ appears suggesting the adherence of surfactant layer on the EgSP surface. However, a decrease in the intensities of the peaks of hydroxyl functional group has been observed on surfactant modification. Thermal

stability of the EgSP based adsorbents has been examined by TGA (Figure 4b), EgSP is showing better stability as compared to the surfactant modified EgSP. The first degradation temperature for EgSP (CaCO_3) is 660°C [16] which shows the purity of the compound and surface modification is also confirmed by the first fall at 280°C .

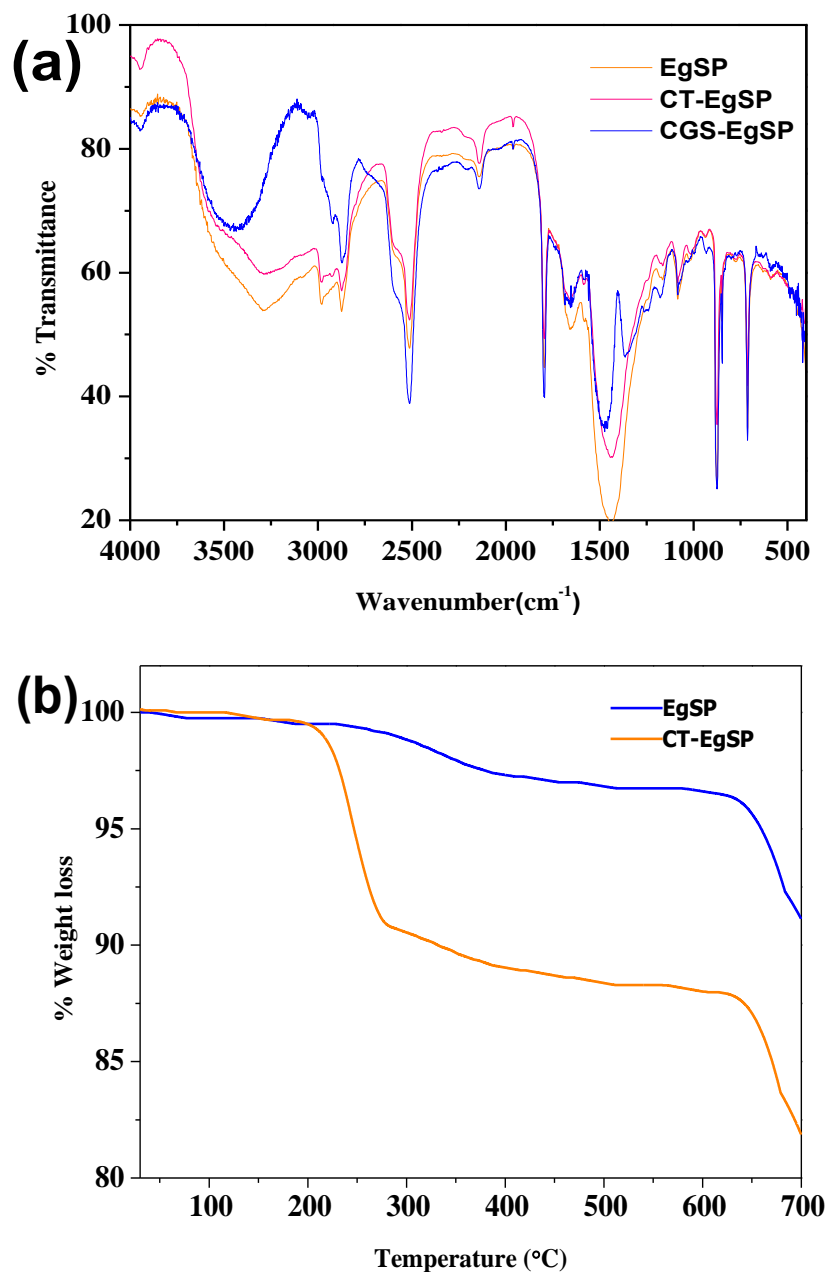


Figure 4. FTIR (a) and TGA (b) plots for EgSP and surfactant modified nanocomposites

2.5. Methodology

2.5.1. Adsorption Studies

Adsorption studies are carried out by batch process. Dye solution (20 mL) of desired concentrations (10–100 mg L⁻¹) were equilibrated with 0.2 g of adsorbents in 50mL capped glass bottle. The mixtures were kept at room temperature for 24 h. Samples after equilibration were taken for UV-VIS analysis. The samples were analyzed in triplicates and adsorption capacity values at equilibrium (q_e) were calculated by using the following relationship:

$$q_e = \left(\frac{C_0 - C_e}{W} \right) \times V \quad (1)$$

where C_0 initial concentration of adsorbate (mg L⁻¹), C_e equilibrium adsorbate concentration (mg L⁻¹), V volume of the solution (L) and W mass of the adsorbent (g).

2.5.2. UV-Visible Spectroscopy

UV-visible spectrophotometer (Shimadzu, UV-2450), equipped with a quartz cell of path length 1cm, was used for absorption measurements of different samples against suitable blanks in the wavelength range of 200-800 nm. Absorption data were acquired for dyes before/after adsorption (Chapter 3) and for solubilization of PAHs (Chapters 4 and 6).

2.5.3. Electric Conductivity Measurements

Conductometric measurements have been carried out by using a conductivity meter EUTECH cyberscan CON510 (cell constant 1 cm⁻¹) with an inbuilt temperature sensor.

A pre-calibrated conductivity cell was used to obtain κ within an appropriate concentration range. Temperature of the sample solution was precisely controlled by SCHOTT CT 1650 thermostat with an accuracy of $\pm 0.1^\circ\text{C}$. The cell with an initial amount of water (30 ml) in a vessel was thermostated for at least 30 minutes prior to

the measurements. The conductivity runs were carried out by adding concentrated surfactant/mixed surfactant(s) solution to the thermostated titrating vessel. cmc values for different surfactants were determined from the intersection point between two straight lines in the plot of the [surfactant] vs. κ .

2.5.4. Surface Tension Measurements

Tensiometric measurements are carried out using Du-Nouy Tensiometer (Model No-STT-78; manufactured by S. C. Dey and Co, Calcutta INDIA) adopting the ring detachment technique at a controlled temperature ($30 \pm 0.1^\circ\text{C}$). Prior to detachment, the platinum ring with gold joints was carefully lifted. Thorough stirring followed by a 10 min interval for equilibration was allowed after each addition. γ Values were directly noted from the instrument accurately within a limit of 0.1 Nm^{-1} . γ vs [surfactant] plot was used to ensure purity (absence of minimum) as well as for the determination of cmc.

2.5.5. NMR Measurement

^1H NMR spectra were obtained with Bruker Avance 400 NMR spectrometer with a proton resonance frequency of 400.15 MHz at 298 K. All the surfactant solutions were prepared in D₂O. About 0.6 ml of solution was transferred to a 5 mm NMR tube and chemical shifts were recorded on the ppm scale. All the spectra are calibrated with the HOD signal at 4.69 ppm (δ). All NMR data were processed using the software package Bruker Topspin 2.1.

2.5.6. Cloud Point (CP) Measurement

Cloud point (CP) data are acquired by placing samples, containing anionic gemini surfactant (12-4-12A) in a fixed [SAIL], into a temperature-controlling thermostatic (SCHOTT CT 1650) water bath. The temperature of the bath was precisely controlled with an accuracy of $\pm 0.1^\circ\text{C}$. Bath temperature was gradually increase and appearance

of the solution was checked after each temperature increment. The first appearance of the turbidity in the sample was taken the cloud point. However, for each sample the procedure was repeated thrice and final CP value was decided on the basis of two identical values (± 0.1 °C).

2.5.7. Polarising Optical Microscopy

Micellar aggregates are visualized by Polarizing optical microscope (POM), Nikon eclipse Ci POL, fitted with Linkem heating stage, was used. Micrographs were obtained either by changing the sample temperature (Chapter 4) or by changing composition of the surfactant mixture (Chapter 5).

2.5.8. Transmission Electron Microscopy

Transmission electron microscope (TEM) of JEOL, Japan (JEM 2100) has been used (accelerating at a working voltage of 120kV) to obtain aggregate images. A drop of the sample solution was placed on the carbon-coated copper grid (200 mesh) followed by drying for a few minutes (~298 K). Later on, a drop of fresh uranyl acetate solution was put on the grid having the dried sample. The grid was again dried at the same temperature and placed in the grid holder. The images were captured through a computer added program provided by the supplier.

2.5.9. SANS Measurements

SANS measurements are carried out using a SANS spectrometer at Dhruva Reactor, Bhabha Atomic Research Centre, Trombay, India [17]. The samples were placed in a quartz cuvette having a thickness of 2 mm and measurements were performed at different compositions / temperatures. Coherent differential scattering cross-section per unit volume ($d\Sigma/d\Omega$), as a function of scattering vector ($Q = 4\pi\sin\theta/\lambda$, where 2θ is the scattering angle and λ is the wavelength of the incoming neutrons), has been measured. For a mono-disperse aggregate, $d\Sigma/d\Omega$ can be given as [18]

$$\frac{d\Sigma}{d\Omega} = n P(Q) S(Q) + B \quad (2)$$

where, n is the particle number density. $P(Q)$ is the form factor and is decided by the shape and size of the particle. $S(Q)$ is the inter-particle structure factor govern by the inter-micellar interactions. B denotes the incoherent scattering background mainly resulted from the hydrogen containing moieties in the aggregates. [19-23].

2.5.9.1. SANS Analysis

In a typical SANS measurement, coherent differential scattering cross-section per unit volume ($d\Sigma/d\Omega$), as a function of scattering vector ($Q = 4\pi \sin \theta/\lambda$, where 2θ is the scattering angle and λ is the wavelength of the incoming neutrons), is measured.

$P(Q)$ for spherical particles of radius R can be given by

$$P(Q) = \frac{16\pi^2}{9} (\rho_p - \rho_s)^2 R^6 \left[3 \frac{\sin(QR) - (QR)\cos(QR)}{(QR)^3} \right]^2 \quad (3)$$

where ρ_p and ρ_s are the scattering length densities of particle and solvent respectively.

For prolate ellipsoidal particles, $P(Q)$ can be expressed as

$$P(Q) = \frac{16\pi^2}{9} (\rho_p - \rho_s)^2 (ab^2)^2 \int_0^1 [F(Q, \mu)]^2 d\mu \quad (4)$$

where functions are given by

$$F(Q, \mu) = \frac{3(\sin x - x \cos x)}{x^3} \quad (5)$$

and $x = Q[a^2\mu^2 + b^2(1-\mu^2)]^{1/2}$, where a and $b=c$ are, respectively semi-major and semi-minor axes of prolate ellipsoid ($a>b=c$). The variable μ is the cosine of the angle between the directions of a and Q .

The following expression provides $P(Q)$ for a spherical core-shell structure,

$$P(Q) = \frac{16\pi^2}{9} [(R+dR)^3 (\rho_{shell} - \rho_s) \frac{\sin Q(R+dR) - Q(R+dR)\cos Q(R+dR)}{Q^3(R+dR)^3} - R^3 (\rho_{shell} - \rho_{core}) \frac{\sin QR - QR\cos QR}{Q^3 R^3}]^2 \quad (6)$$

where R is core radius and dR is shell thickness. ρ_{core} and ρ_{shell} represents the scattering length densities of the core and shell, respectively.

$S(Q)$ is the Fourier transform of the radial distribution function $g(r)$ for the mass centers of the particles and hence correlates particles present in the system. For charged micellar system, $S(Q)$ is calculated by using the Hayter and Penfold analysis under rescaled mean spherical approximation (RMSA) which assumes screened Coulomb interaction between the charged particles. For dilute samples, $S(Q)$ may be approximated to unity.

The repulsive interactions between micelles give rise to a correlation peak which is related to the inter-micellar distance. An empirical formula which correlates peak position with the distance between the micelles (D) is given by

$$Q_p D = 6.8559 + 0.0094D \quad (7)$$

Throughout the data analysis corrections were made for instrumental smearing. The calculated scattering profiles were smeared by the appropriate resolution function to compare with the measured data. The parameters in the analysis were optimized by means of a nonlinear least-square fitting program, namely, sasfit.

2.5.10 Dynamic Light Scattering (DLS) / Zeta (ζ)-Potential Measurements

Average hydrodynamic diameter (D_h) and Zeta (ζ) - potential measurements were performed on a SZ-100 nanoparticle size analyzer (HORIBA, Japan). This instrument is equipped with a green (5320Å) laser and photomultiplier tube detectors. The measurement is based on the time dependent fluctuation in the intensity of scattered light through a dispersion of particles under random motion. Analysis allows to compute diffusion coefficients which are used in Stokes-Einstein equation for the determination of D_h .

2.5.11. Solubilization Experiment

Solubility of PAH has been determined in aqueous surfactant systems (single or mixed), by adding an excess amount of PAH (fluorene, anthracene, phenanthrene or pyrene). Aqueous surfactant(s) + PAH mixture has been equilibrated for 48h before centrifugation to remove excess PAH. The solubilization of PAH in micellar solutions, containing different morphologies, has been analysed, at respective λ_{max} , by UV-visible spectrophotometer mentioned in section 2.3.2. The composition of surfactant mixture was same in both reference and measurement cuvettes (to eliminate its effect on the UV-absorbance). Absorbance (A) data have been used to determine [PAH] (and hence molar solubility) using Lambert-Beer Law. The molar solubilization ratio (MSR) is the ratio of the molar solubility of the PAH in micelles to the total [gemini(s)] in the micellar form [24]. MSR can be computed by the following expression,

$$MSR = \frac{(S_t - S_{cmc})}{(C_t - C_{cmc})} \quad (8)$$

where, S_t is the total PAH molar solubility in the aqueous gemini mixture at fixed [surfactant] ($C_t=10$ mM). S_{cmc} is the solubility of the PAH corresponding to the cmc

of the gemini mixture (C_{cmc}). Same procedure has been adopted in the co-solubilization experiment where more than one PAHs were solubilized simultaneously.

References

- [1] M. J. Rosen, *Chemtech*. 23 (1993) 30;
- [2] F. M. Menger, J. S. Keiper, *Angew Chem. Int. Ed.* 39 (2000) 1906, and references there in;
- [3] R. Zana, *Adv. Colloid Interface Sci.* 97 (2002) 205-253.
- [4] A. K. Nelson, A. D. F. Toy, *Inorg. Chem.* 2, 1963, 775-777.
- [5] R. A. Bauman, *Synthetic Comm.* 1974, 870;
- [6] S. De, V. K. Aswal, P. S. Goyal, S. Bhattacharya, *Chem. Phys. Letter.* 1999, 303, 295-303.
- [7] W.S. Hummers Jr, R.E. Offeman, *J. Am. Chem. Soc.* 1958, 80, 1339-1339;
- [8] K.B. Dhopte, R.S. Zambare, A.V. Patwardhan, P.R. Nemade, *RSC Adv.* 2016, 6, 8164-8172.
- [9] R.A.K. Rao, S. Singh, B.R. Singh, W. Khan, A. Naqvi, , *J. Environ. Chem. Eng.* 2014, 2 ,199-210;
- [10] B.R. Singh, M. Shoeb, W. Khan, A.H. Naqvi, , *J. Alloys and Compd*, 2015, 651, 598-607.
- [11] N.M. Mahmoodi, S.M. Maroofi, M. Mazarji, G. Nabi-Bidhendi, *J. Surf. Deterg.* 2017, 20, 1085-1093.
- [12] F. Li, M. Rosen, *J. Colloid. Interf. Sci.* 2000, 224, 265-271.
- [13] M. Rosen, F. Li, *J. Colloid. Interf. Sci.* 2001, 234, 418-424.
- [14] W.T. Tsai, K.J. Hsien, H.C. Hsu, C. M. Lin, K.Y. Lin and C.W. Yeh, *Bioresource Technol.* 2008, 99, 1623-1629.
- [15] M. Arami, N. Y. Limaee and N.M. Mahmoodi, *Chemosphere*, 2006, 65, 1999-2008.
- [16] S.K. Swain, S. Dash, S.K. Kisku and R.K. Singh, *Mater. Sci. Technol.*, 2014, 30, 791-795
- [17] V. Aswal, P. Goyal, *Current Science* 2000, 79, 947-953.
- [18] D.I. Svergun, M.H. Koch, *Rep. Prog. Phys.* 2003, 66,1735
- [19] J.S. Pedersen, *Adv. Colloid. Interf. Sci.* 1997, 70, 171-210.
- [20] J.B. Hayter, J. Penfold, *Mol. Phys.* 1981, 42, 109-118
- [21] S. Chen, E.Y. Sheu, J. Kalus, H. Hoffman, *J. Appl. Crystallogr* 1988, 21, 751-769.

- [22] I. Breßler, J. Kohlbrecher, A.F. Thünemann, *J. Appl. Crystallogr.* 2015, 48, 1587-1598.
- [23] R. Kaur, S. Kumar, V.K. Aswal, R.K. Mahajan, , *Langmuir*, 2013, 29, 11821-11833.
- [24] D. A. Edwards, R.G. Luthy, Z. Liu, *Environ. Sci. Technol.* 1991, 25,127-133.